Comparison of Spatial Variability in Visible and Near-Infrared Spectral Images

Pat S. Chavez, Jr.
U. S. Geological Survey, 2255 North Gemini Drive, Flagstaff, AZ 86001

ABSTRACT: The visible and near-infrared bands of the Landsat Thematic Mapper (TM) and the Satellite Pour l'Observation de la Terre (SPOT) were analyzed to determine which band contained more spatial variability. It is important for applications that require spatial information, such as those dealing with mapping linear features and automatic image-to-image correlation, to know which spectral band image should be used. Statistical and visual analyses were used in the project. The amount of variance in an 11 by 11 pixel spatial filter and in the first difference at the six spacings of 1, 5, 11, 23, 47, and 95 pixels was computed for the visible and near-infrared bands. The results indicate that the near-infrared band has more spatial variability than the visible band, especially in images covering densely vegetated areas.

INTRODUCTION

HISTORICALLY, MONOCHROMATIC IMAGES have been collected using primarily the visible portion of the spectrum. With the advent of multispectral imaging systems, image data are now routinely collected in several spectral bands, giving the user more options for data analyses and interpretation. These image data contain information about the spectral and spatial characteristics of the surface being viewed. The spectral information contents of the Landsat Thematic Mapper (TM) and the Satellite Pour l'Observation de la Terre (SPOT) have been discussed previously (Chavez and Bowell, 1988). The differences and possible combinations of the spectral information in the visible and near-infrared bands have also been investigated (Tucker, 1979; Gallo and Eidenshink, 1988). Studies have been made also of both the spatial variation of vegetation changes at very coarse scales and the factor of scale in remotely sensed image data (Townshend and Justice, 1990; Woodcock and Strahler, 1987).

The study discussed in this paper was concerned with the spatial information in remotely sensed multispectral image data, particularly in the visible and near-infrared spectral bands. The objective of this study was to compare the visible and near-infrared spectral bands from a spatial information point of view. The results of the comparison showed that the near-infrared band contains more spatial information than the visible band. Therefore, applications dealing with mapping linear features, such as faults, and automatic image-to-image digital matching, such as for multitemporal geometric registration or stereo compilation for the extraction of topographic information, will benefit from using a near-infrared spectral band rather than a visible band. The amount of spatial variability was analyzed at both the local and regional scales using a spatial filter and first differences of the image data. The comparison was made between the visible and near- infrared bands collected by the same sensor, with the same spatial resolution, at the same time. Therefore, any differences in the amount of spatial variation should be due to the spectral bands, and not the sensor characteristics or spatial resolution used to collect the data.

DATA CHARACTERISTICS AND TEST SITES

In order to evaluate the spatial variability in the visible and near-infrared spectral bands, six sites of different geographic conditions were analyzed. The image data for four of the sites were collected by SPOT and distributed in the Education and Evaluation Data Set (SEEDS) package. These data have a spatial resolution of 20 m in two visible wavelength bands and one near-infrared band. The two SPOT bands used in the analyses were bands XS1 and XS3, which correspond roughly to the green and near-infrared portions of the spectrum – 0.50 to 0.59 and 0.79 to 0.89 micrometres, respectively. The image data for the other two sites were collected by the Landsat TM; these data have a spatial resolution of 30 m in six spectral bands (excluding the 120-m thermal band). The two spectral bands used were TM2 and TM4, which also correspond roughly to the green and near-infrared portions of the spectrum – 0.52 to 0.62 and 0.76 to 0.90 micrometres, respectively. The spectral bands of the two systems are not identical; however, this was not relevant because the comparison was between the visible and near-infrared portions of the spectrum and not between the two imaging sensors.

The four sites covered by the SPOT data were (1) Pilar, Paraguay, (2) Rift Valley, Kenya, (3) Toulouse, France, and (4) Bangkok, Thailand. The remaining two sites, covered by the Landsat TM data, were (5) the north rim of the Grand Canyon, Arizona and (6) the mountains south of San Francisco, California. In the color composites of the six sites shown in Plate 1, the green, red, and near-infrared spectral bands were exposed through the blue, green, and red filters, respectively; in this combination vegetation is red. The areas covered by the four SPOT images are 10.2 km per side and the TM images cover areas of 15.4 km per side (512 by 512 pixels). The following descriptions are for the sites shown in Plate 1; the descriptions for the SPOT images were extracted from the information supplied with the SPOT SEEDS package. The Pilar, Paraguay image (Plate 1a) acquired on 27 March 1986, shows the meandering Paraguay river with surrounding swamps and highly forested areas. The Rift Valley, Kenya image (Plate 1b) acquired on 14 March 1986, shows how the deforestation follows the valleys upstream, with the only area of native forest in the upper right part of the image. The crops had just been planted so the fields appear as bare soil rather than vegetated. The Toulouse, France image (Plate 1c) was acquired on 22 May 1986. The city is mostly on the left side of the image, with the Garonne River and the Canal de Midi going through the center; the right side shows mostly an agricultural environment. The Bangkok, Thailand image (Plate 1d) acquired on 10 March 1986, shows mostly rice paddies in various shades of red or blue; the areas in red correspond to paddies where water has retreated and those in blue to areas where the paddies are still flooded. Plate 1e, the image of the north rim of the Grand Canyon, acquired on 24 August 1985, shows some of the drainage patterns on top of the north rim that has both Ponderosa pine and Juniper trees. Plate 1f is an image of a mountainous area that is approximately 40 km south of San Francisco; the image was acquired on 31 December 1982. The mountains are covered mostly with coniferous and deciduous

PHOTOGRAMMETRIC ENGINEERING & REMOTE SENSING,
Vol. 58, No. 7, July 1992, pp. 957–964.

0099-1112/92/5807-957$03.00/0

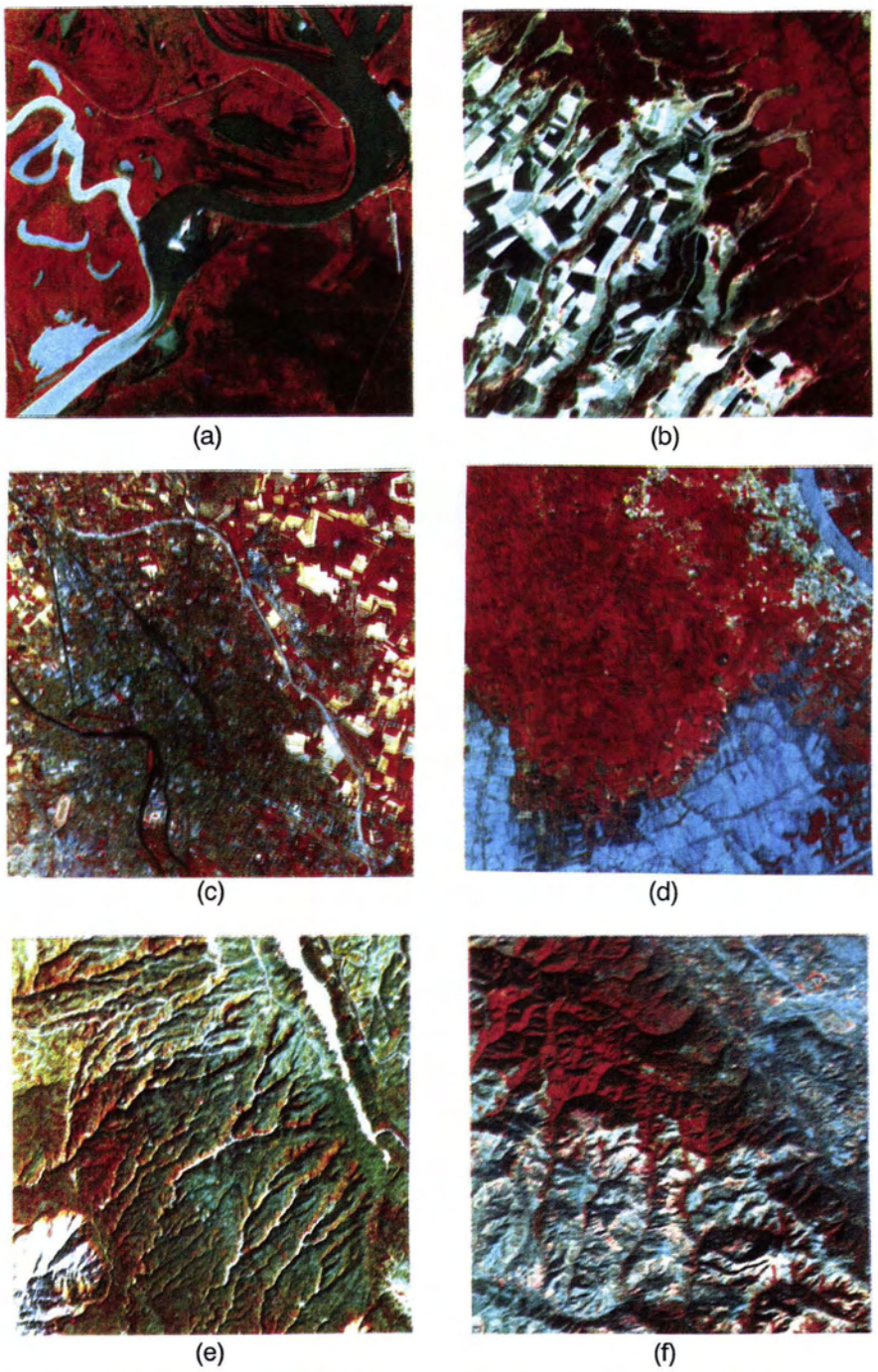

PLATE 1. False color composite images made with the near-infrared band throught the red filter so that vegetation is red and soils and water are in various shades of blue. Images (a), (b), (c), and (d) were collected by the SPOT and (e) and (f) were collected by the Landsat TM. Each digital array had 512 by 512 pixels. so that the images are approximately 10.2 km on a side for the SPOT data and 15.4 km on a side for the Landsat TM data. (a) Pilar, Paraguay. (b) Rift Valley, Kenya. (c) Toulouse, France. .(d) Bangkok, Thailand. (e) Grand Canyon. (f) San Francisco. (SPOT image copyright 1991 CNES.)

trees (of course, in December the deciduous trees do not have any leaves).

ANALYSES OF THE DATA

To compare the visible and near-infrared spectral bands from a spatial information point of view, the amount of spatial variability in these two bands was analyzed using statistical and visual methods. As mentioned previously, only the green and near-infrared spectral bands were used (SPOT XS 1 and 3 and TM 2 and 4) and no cross comparisons between the SPOT and TM data were made. The standard deviations and image results of an 11- by 11-pixel high pass filter (HPF) applied to the visible and near-infrared bands were compared. Also, the variance/

standard deviation of the first difference at six spacings/scales were computed and analyzed.

The 11 by 11 HPF was a Laplacian type spatial filter that subtracts the average of the 11 by 11 window from the center pixel. An offset of 127 is automatically added to keep the data centered in the 0 to 255 digital number (DN) range. The 11 by 11 kernel was used because it included spatial information at both the local and intermediate scales, and it showed the trend of the regional scale results. The graphs of the first differences at the spacings of 1, 5, 11, 23, 47, and 95 pixels will show how the 11-pixel spacing compares with these other kernel sizes. The results of the HPF show how a pixel differs from its neighbors (i.e., the pixel's spatial variability with its surrounding area). The more variable an image is spatially, the larger will be the variance of the HPF results; the more homogeneous an area is, the less variable it will be spatially and, therefore, the variance will be smaller.

Table 1 shows the standard deviation of the HPF results for the visible and near-infrared bands for the six sites. Also shown are the values of the ratio of the standard deviation of the near-infrared to visible HPF results. This parameter is useful because it shows the difference in the amount of variation in one band versus the other. The larger the standard deviation the more spatially variable an image is, and the larger the ratio between the two bands the more spatially variable the near-infrared band is compared to the visible band. The ratio values show in quantitative terms the amount of "more" spatial variability in the near-infrared band as compared with the visible band. A value of 1 indicates the same amount of spatial variability in both bands. Because of the differences between the SPOT and TM systems, the results should not be compared with each other; only sites collected by the same imaging system should be compared with each other. The image results of the 11 by 11 HPF applied to the visible and near-infrared bands are shown in Figures 1a to 1f. For visual comparison and analysis, all the images had a 1 and 99 percent contrast stretch applied. This was done to give all the images the same amount of contrast for the visual comparison, but it should be noted that the dynamic range of the visible compared with the near-infrared HPF results is very important. The difference in dynamic range is given by the differences in their standard deviations shown in Table 1.

Of the four image data sets collected by SPOT, the Paraguay site not only had the largest standard deviation in the near-infrared band, it also had the largest ratio between the two bands. As can be seen from the color composites shown in Plate 1, Pilar (Plate 1a) is a very densely vegetated site. The Bangkok image (Plate 1d) had the second largest ratio between the near-infrared and visible bands; however, the values of the individual standard deviations were smaller than the remaining two SPOT images (France and Kenya images, Plates 1c and 1b, respectively). For the two sites covered by Landsat TM data, the site on the north rim of the Grand Canyon had a larger standard deviation than the site south of San Francisco, but the image covering the mountains south of San Francisco had the larger ratio. At all six sites the ratio of the standard deviation of the near-infrared to the visible was greater than 1, implying that at the 11- by 11-pixel window/scale there was more spatial variability in the near-infrared band. The ratio ranged from 1.3 to 3.6 for the SPOT data and 2.6 to 4.6 for the TM data.

TABLE 1. STANDARD DEVIATION VALUES OF THE RESULTS OF THE HIGH PASS FILTERS (HPFS) APPLIED TO THE VISIBLE AND NEAR-INFRARED BANDS OF BOTH THE SPOT AND TM DATA FOR THE SIX SITES. THE KERNAL SIZE OF THE HPF WAS 11 BY 11 PIXELS. ALSO SHOWN ARE THE RATIOS OF THE STANDARD DEVIATIONS OF THE NEAR-INFRARED (XS3 OR TM4) TO THE VISIBLE (XS1 OR TM2) BANDS.

	SPOT Data				TM Data	
	Paraguay	Kenya	France	Bangkok	Grand Canyon	San Francisco
Visible	3.0	5.1	4.9	1.7	3.2	1.5
Near-IR	10.9	6.8	7.0	4.3	8.3	6.9
NIR/VIS	3.6	1.3	1.4	2.5	2.6	4.6

Visual comparison of the HPF images substantiates the values shown in Table 1; that is, the near-infrared band has more detail/high frequencies, therefore, more spatial variability, than does the visible band (see Figure 1). All the images have approximately the same amount of contrast because of the 1 and 99 percent stretch applied to the HPF images; this was done to help with the display and visual analyses of the data. Upon close examination it becomes clear that the near-infrared band does have more spatial detail; this is especially obvious in the more densely vegetated areas. Some subareas appear to have more spatial variability in the visible band than in the near-infrared band; these areas include some urban features and certain types of roads. However, overall, the near-infrared band has more spatial variability than the visible band, as indicated by the standard deviations shown in Table 1.

The analyses by the HPF method considered the spatial variability at only one scale (11 by 11 pixels). The first difference, which approximates the first derivative, at six different spacings was used to examine the spatial variability at several different scales (i.e., local to regional). The spacings used between pixels to take the first difference were 1, 5, 11, 23, 47, and 95 pixels. These spacings were selected in order to analyze the spatial variations from the local to regional scales. The actual spacing size used was not important; the trend of spatial variability from the local to regional scales was the information that was critical. The standard deviation at each spacing, the ratio between adjacent spacings, and the ratio of the near-infrared to the visible bands were computed. The results for the six sites are shown in Tables 2 to 7. The graphs shown in Tables 2 to 7 were generated by plotting the standard deviation of the first difference in the horizontal direction at the five spacings of 1, 5, 11, 23, and 47 pixels. The resulting plots show the spatial characteristics of the image data at these five scales. Note that the plots in the tables look similar to those generated by semivariogram analysis. This similarity is to be expected because the algorithm used to compute the semivariograms includes the first difference (Woodcock, 1985; Curran, 1988). In the graphs shown in Tables 2 to 7, the entire image was used, rather than subareas of individual cover types, to compute the variance at each spacing, or "lag," in semivariogram language. The graphs for the two TM images, Grand Canyon and San Francisco, flatten out at about the 11-pixel spacing, and two of the SPOT images, Kenya and France, flatten out at about the 23-pixel spacing. In semivariogram analysis, these pixel locations/lags are called the "range," and their corresponding variance is called the "sill." In this study the first difference was used because it is more efficient and easier to use, and was sufficient to extract the spatial variability information required for this study.

By comparing the standard deviation at each spacing and the ratio of adjacent spacings, the rate of spatial variability change as a function of distance can be seen. The ratio of the near-infrared to the visible standard deviations shows how much more, or less, the spatial variability is in one band compared with the other. If this ratio is greater than 1, the near-infrared band is more spatially variable than the visible band; if less than 1, the near-infrared band is less spatially variable than the visible band. To help in the analyses of these data, graphs of the standard deviations of the near-infrared and visible bands at the first five spacings are shown in Tables 2 to 7. The sample increment/spacing (horizontal axis) is constant for all six graphs/

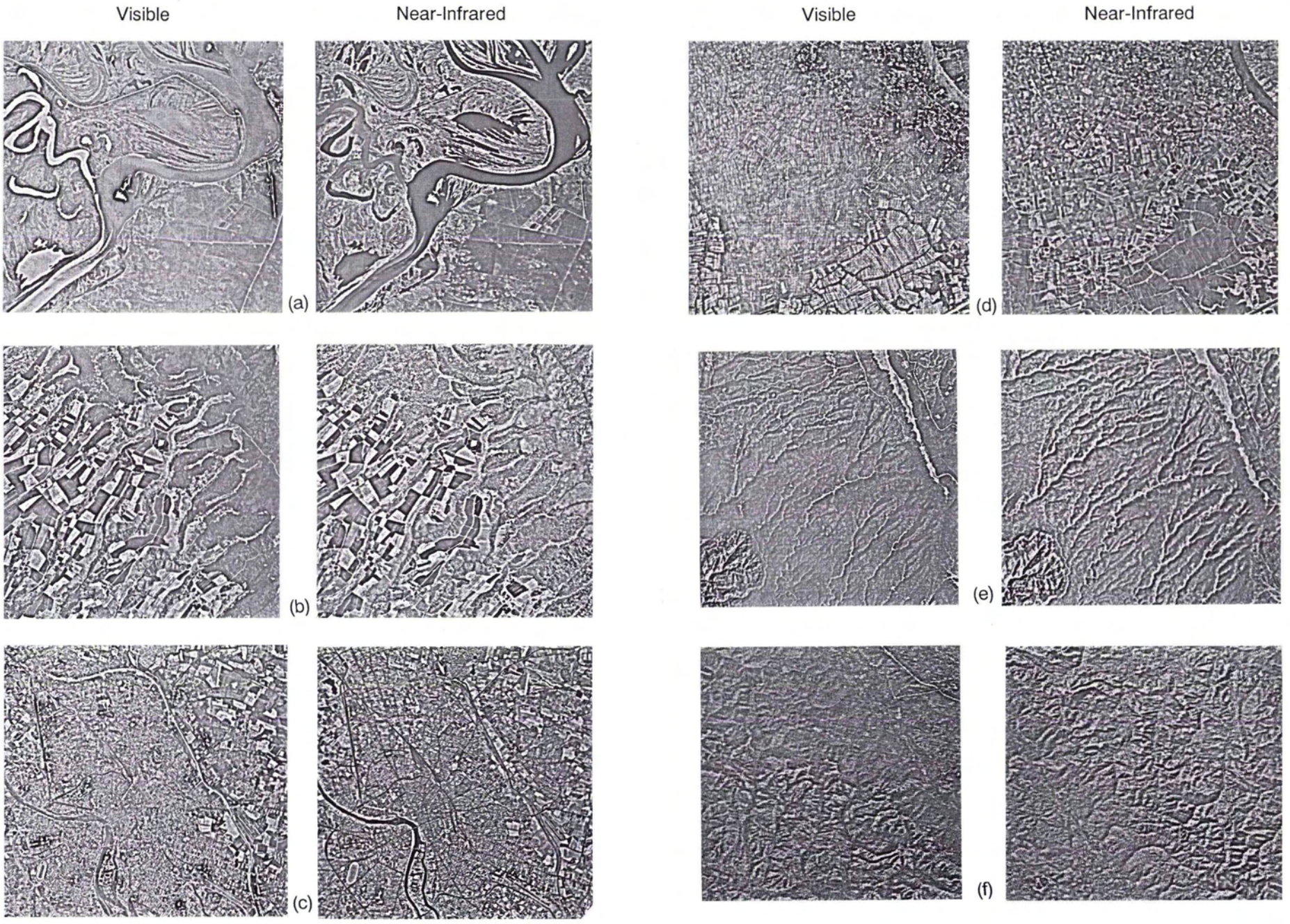

FIG. 1. Image results of the 11- by 11-pixel high pass filter (HPF) applied to the visible (left) and near-infrared (right) bands. A 1 and 99 percent linear stretch was applied to all the images so that they would have approximately the same amount of contrast for the visual analyses. The order and scale of the images are the same as those shown in Plate 1. (a) Pilar, Paraguay. (b) Rift Valley, Kenya. (c) Toulouse, France. (d) Bangkok, Thailand. (e) Grand Canyon. (f) San Francisco. (SPOT image copyright 1991 CNES.)

TABLE 2. PILAR, PARAGUAY. STANDARD DEVIATION (SD) VALUES OF RESULTS OF THE HORIZONTAL FIRST DIFFERENCES, WHICH APPROXIMATE THE FIRST DERIVATIVES, AT SIX SPACING INTERVALS APPLIED TO THE VISIBLE AND NEAR-INFRARED BANDS, AND RATIOS OF SD VALUES FOR ADJACENT INTERVALS IN INCREASING ORDER AND THE SD OF NEAR-INFRARED TO VISIBLE. SPACING INTERVALS 1, 5, 11, 23, 47, AND 95 PIXELS WERE USED TO TAKE THE FIRST DIFFERENCE.

	VISIBLE (XS1)		NEAR-INFRARED (XS3)		
Sample Increment	Standard Deviation	Ratio (ith+1)/ith	Standard Deviation	Ratio (ith+1)/ith	Ratio NIR/VIS
1	2.29	2.36	6.85	2.75	2.99
5	5.40	1.34	18.81	1.30	3.48
11	7.23	1.16	24.49	1.20	3.39
23	8.42	1.10	29.36	1.12	3.49
47	9.22	0.98	32.99	1.05	3.58
95	9.01	----	34.55	----	3.83

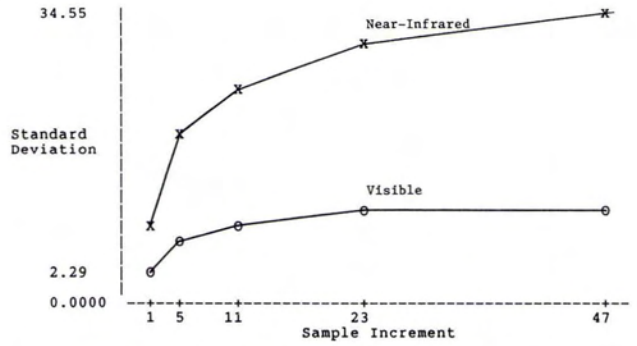

Standard deviations of the visible and near-infrared bands for the first five spacings.

TABLE 3. RIFT VALLEY, KENYA. STANDARD DEVIATION (SD) VALUES OF RESULTS OF THE HORIZONTAL FIRST DIFFERENCES, WHICH APPROXIMATE THE FIRST DERIVATIVES, AT SIX SPACING INTERVALS APPLIED TO THE VISIBLE AND NEAR-INFRARED BANDS, AND RATIOS OF SD VALUES FOR ADJACENT INTERVALS IN INCREASING ORDER AND THE SD OF NEAR-INFRARED TO VISIBLE. SPACING INTERVALS 1, 5, 11, 23, 47, AND 95 PIXELS WERE USED TO TAKE THE FIRST DIFFERENCE.

	VISIBLE (XS1)		NEAR-INFRARED (XS3)		
Sample Increment	Standard Deviation	Ratio (ith+1)/ith	Standard Deviation	Ratio (ith+1)/ith	Ratio NIR/VIS
1	3.70	2.53	4.61	2.66	1.25
5	9.36	1.34	12.26	1.33	1.31
11	12.52	1.17	16.33	1.15	1.30
23	14.60	1.02	18.84	1.02	1.29
47	14.90	1.03	19.25	1.04	1.29
95	15.32	----	20.04	----	1.31

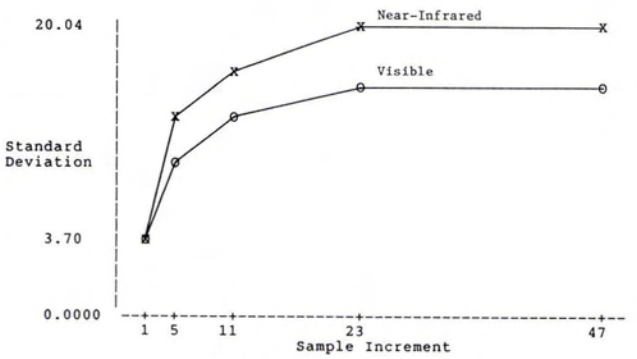

Standard deviations of the visible and near-infrared bands for the first five spacings.

TABLE 4. TOULOUSE, FRANCE. STANDARD DEVIATION (SD) VALUES OF RESULTS OF THE HORIZONTAL FIRST DIFFERENCES, WHICH APPROXIMATE THE FIRST DERIVATIVES, AT SIX SPACING INTERVALS APPLIED TO THE VISIBLE AND NEAR-INFRARED BANDS, AND RATIOS OF SD VALUES FOR ADJACENT INTERVALS IN INCREASING ORDER AND THE SD OF NEAR-INFRARED TO VISIBLE. SPACING INTERVALS 1, 5, 11, 23, 47, AND 95 PIXELS WERE USED TO TAKE THE FIRST DIFFERENCE.

	VISIBLE (XS1)		NEAR-INFRARED (XS3)		
Sample Increment	Standard Deviation	Ratio (ith+1)/ith	Standard Deviation	Ratio (ith+1)/ith	Ratio NIR/VIS
1	3.87	2.02	4.82	2.39	1.25
5	7.80	1.10	11.50	1.15	1.47
11	8.60	1.06	13.26	1.06	1.54
23	9.10	1.01	14.00	1.07	1.54
47	9.23	1.01	14.96	1.09	1.62
95	9.31	----	16.27	----	1.75

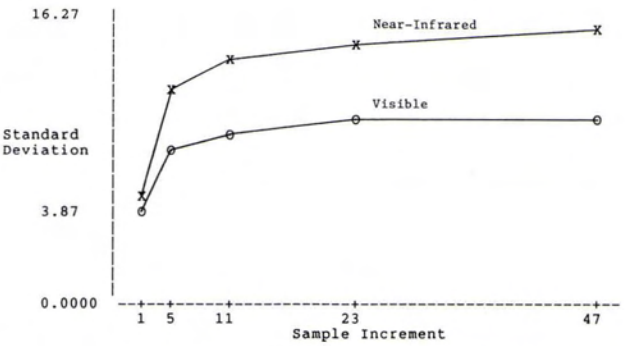

Standard deviations of the visible and near-infrared bands for the first five spacings.

TABLE 5. BANGKOK, THAILAND. STANDARD DEVIATION (SD) VALUES OF RESULTS OF THE HORIZONTAL FIRST DIFFERENCES, WHICH APPROXIMATE THE FIRST DERIVATIVES, AT SIX SPACING INTERVALS APPLIED TO THE VISIBLE AND NEAR-INFRARED BANDS, AND RATIOS OF SD VALUES FOR ADJACENT INTERVALS IN INCREASING ORDER AND THE SD OF NEAR-INFRARED TO VISIBLE. SPACING INTERVALS 1, 5, 11, 23, 47, AND 95 PIXELS WERE USED TO TAKE THE FIRST DIFFERENCE.

	VISIBLE (XS1)		NEAR-INFRARED (XS3)		
Sample Increment	Standard Deviation	Ratio (ith+1)/ith	Standard Deviation	Ratio (ith+1)/ith	Ratio NIR/VIS
1	1.34	1.96	2.85	2.45	2.13
5	2.63	1.15	6.98	1.17	2.65
11	3.02	1.11	8.16	1.11	2.70
23	3.35	1.15	9.02	1.12	2.69
47	3.86	1.19	10.06	1.14	2.61
95	4.60	----	11.49	----	2.50

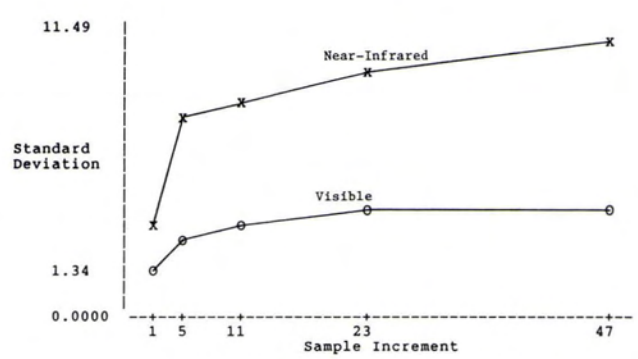

Standard deviations of the visible and near-infrared bands for the first five spacings.

TABLE 6. GRAND CANYON, ARIZONA. STANDARD DEVIATION (SD) VALUES OF RESULTS OF THE HORIZONTAL FIRST DIFFERENCES, WHICH APPROXIMATE THE FIRST DERIVATIVES, AT SIX SPACING INTERVALS APPLIED TO THE VISIBLE AND NEAR-INFRARED BANDS, AND RATIOS OF SD VALUES FOR ADJACENT INTERVALS IN INCREASING ORDER AND THE SD OF NEAR-INFRARED TO VISIBLE. SPACING INTERVALS 1, 5, 11, 23, 47, AND 95 PIXELS WERE USED TO TAKE THE FIRST DIFFERENCE.

	VISIBLE (XS1)		NEAR-INFRARED (XS3)		
Sample Increment	Standard Deviation	Ratio (ith+1)/ith	Standard Deviation	Ratio (ith+1)/ith	Ratio NIR/VIS
1	2.60	2.00	6.21	2.26	2.39
5	5.20	1.17	14.03	1.18	2.70
11	6.06	1.06	16.55	1.03	2.73
23	6.45	0.99	16.97	1.00	2.63
47	6.41	1.04	16.98	1.00	2.65
95	6.64	----	16.90	----	2.55

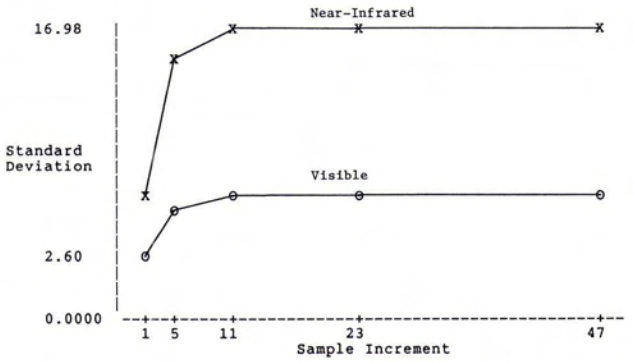

Standard deviations of the visible and near-infrared bands for the first five spacings.

TABLE 7. SAN FRANCISCO, CALIF.STANDARD DEVIATION (SD) VALUES OF RESULTS OF THE HORIZONTAL FIRST DIFFERENCES, WHICH APPROXIMATE THE FIRST DERIVATIVES, AT SIX SPACING INTERVALS APPLIED TO THE VISIBLE AND NEAR-INFRARED BANDS, AND RATIOS OF SD VALUES FOR ADJACENT INTERVALS IN INCREASING ORDER AND THE SD OF NEAR-INFRARED TO VISIBLE. SPACING INTERVALS 1, 5, 11, 23, 47, AND 95 PIXELS WERE USED TO TAKE THE FIRST DIFFERENCE.

	VISIBLE (XS1)		NEAR-INFRARED (XS3)		
Sample Increment	Standard Deviation	Ratio (ith+1)/ith	Standard Deviation	Ratio (ith+1)/ith	Ratio NIR/VIS
1	1.67	1.35	7.34	1.39	4.40
5	2.25	1.20	10.17	1.19	4.52
11	2.69	1.09	12.07	1.08	4.49
23	2.92	1.04	13.06	1.03	4.47
47	3.04	1.05	13.40	1.01	4.41
95	3.19	----	13.53	----	4.24

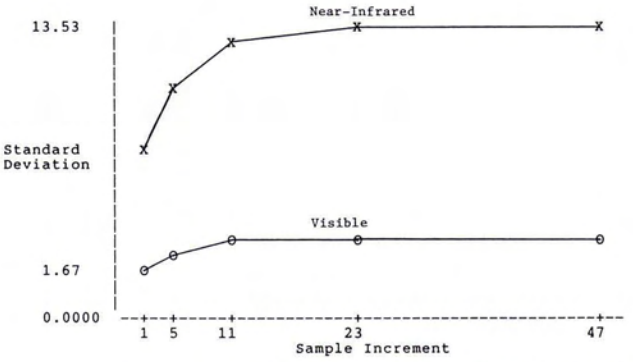

Standard deviations of the visible and near-infrared bands for the first five spacings.

sites; however, the standard deviation (vertical axis) changes from site-to-site because the value used for the maximum is relative only to the particular image represented in the table. The 95-pixel spacing was left off the graph so that the scaling onto the sheet of paper would enable the local to intermediate results to be seen better (i.e., reduced the compression needed to fit the graph on the paper by a factor of two). This was done only because the 95-pixel spacing information is given in the table and the trend in each of the graphs is obvious; nothing is lost by leaving this point off the graphs.

Table 2 shows the results for the image at Paraguay; this site is the most densely vegetated of all. The values of the near-infrared to visible ratio at the six different spacings clearly show that the amount of spatial variability in the near-infrared band is much higher than that in the visible band. This ratio ranges from 2.99 at the local scale to 3.83 at the regional scale. Also, the rate of change is larger for the near-infrared band than for the visible band, especially at the local to intermediate scales. Table 3 shows the results for the image at the Kenya site; more than half the image is bare soils, and the rest is densely vegetated. In this data set, the amplitude of the standard deviations for the visible band are higher than that of the Paraguay site image, but the near-infrared values are lower. However, the values of the near-infrared to visible ratio at the six different spacings still show that the spatial variability in the near-infrared band is higher. The ratio values range from 1.25 to 1.31 for the local and regional scales, respectively. Although the rate of change at the local scale is slightly larger for the near-infrared band, it stays approximately the same for both bands once the spacing is past the local scale.

Table 4 shows the results for the site in France, which is mostly an urban and agricultural site. The standard deviation values for the visible band are in about the same range as the values for the Paraguay site, but the near-infrared values are almost half the values of those of the Paraguay site. But again, the near-infrared values are larger than the visible values so the ratios are all greater than 1. Therefore, the spatial variability in the near-infrared is larger than in the visible band; the range of the ratios is from 1.25 to 1.75 from local to regional scales, respectively. The rate of change at the local scale is about 18 percent higher for the near-infrared compared with the visible band, and the rate levels off towards the more regional scales.

Table 5 shows the results for the image of Bangkok which is mostly an agricultural site. Of the four sites covered by SPOT data, this one had the lowest standard deviation values in both the first difference and HPF results. The four data sets were collected at approximately the same time of year; therefore, differences due to sun-angle effects should not have played a major role in the differences seen from site-to-site; there will be a sun-angle difference due to their latitude differences. Noteworthy with this particular data set is that the visible band (XS1) had considerably more striping noise than the near-infrared band (see Figure 1d) and was the only image with a striping problem. The striping will increase the amount of spatial variability present in the visible band. However, a comparison of the standard deviation and ratio values reveals that the near-infrared band still had more spatial variability than the visible band. The ratio values were 2.13 and 2.50 for the local and regional scales, respectively. For this data set the maximum ratio values occurs at the spacings of 11 and 23 pixels (2.70 and 2.69) rather than at the regional scale of 95 pixels; this was the only SPOT image in which this happened; this may be related to either the striping noise and/or the size of the fields. The rate of change at the local scale was 25 percent larger for the near-infrared band than the visible band, but the rate was approximately the same at the other scales.

Table 6 shows the results for the site on the north rim of the Grand Canyon, which is on a high plateau with large drainage features. The main vegetation types are Ponderosa pine (Pinus

ponderosa) and Juniper trees. The analyses for this and the next site were done with Landsat TM data. A comparison of the values of the standard deviations and ratios of the near-infrared and visible bands shows that the spatial variability is larger in the near-infrared band than in the visible band. The ratio values range from 2.39 to 2.55 for the local and regional scales, respectively. The maximum ratio value, 2.73, occurred at the 11-pixel spacing, and the rate of change was about 13 percent larger for the near-infrared band at the local scale compared to the regional scale; the rate leveled off at about the 11-pixel spacing.

Table 7 shows the results for the site in the mountains south of San Francisco, which is mostly a forested area. This image was collected in December, so the deciduous trees are leafless and the conifers retain their needles (red in Figure 1f). The standard deviation values in the visible band were low, like that of the Bangkok image. Comparing the ratios of the near-infrared to the visible bands shows that the spatial variability is larger in the near-infrared band than in the visible band. The ratio values for the local and regional scales were 4.40 and 4.24, respectively. The regional value was smaller than the local value; the maximum value occurred at the 5-pixel spacing for this data set.

DISCUSSION

Images covering densely vegetated mountainous terrain are often difficult to use because both the dynamic range and amplitude of the radiance for vegetation are low in the visible portion of the spectrum. Therefore, the dynamic range of the DNs in the visible bands is also low, so spatial variability is low, as shown both statistically and visually in the preceding section. In the visible bands the radiance of vegetation is generally low in comparison to that of soils/nonvegetated areas (dark basalts are an exception); therefore, the contrast between the vegetated and nonvegetated areas can be large, often extreme. In the near-infrared bands the radiance of vegetation is high relative to its radiance in the visible bands; its radiance is often similar to that of soils. Therefore, the contrast between vegetated and nonvegetated areas is not as large in the near-infrared bands. The local detail, which includes local topographic variations, often shows up better in the near-infrared band than the visible band because of the lack of this extreme contrast between vegetated and nonvegetated areas. Also, just as important, perhaps more, is that the higher dynamic radiometric range for vegetation in the near-infrared band, as indicated by the larger standard deviations, enables more spatial variations to be detected (i.e., local changes/details will not be quantized together to form a spectrally flat/homogeneous area). This was particularly obvious in the example of the Paraguay site which was the most densely vegetated of all six sites.

The results of this study indicate that applications that require spatial variability information for their analyses should often benefit by using the near-infrared rather than the visible spectral band. For example, the use of image-to-image digital correlation for multitemporal geometric registration or the extraction of topographic information from stereo pairs should generate better results with a near-infrared band than with a visible band, especially in areas that are densely vegetated. This is supported by several previous studies in which authors have found that data collected in the near-infrared band had a higher correlation with topography than data collected in the visible part of the spectrum. In a study using Landsat Multispectral Scanner (MSS) data over a mountainous terrain covered by deciduous woodlands, it was found that MSS bands 4 and 5, approximately the green and red portions of the spectrum, showed no visible topographic effect (Justice *et al.*, 1981). In another study Teillet *et al.* (1982) examined how the radiometric properties of Landsat MSS and an 11-channel airborne MSS over different forest areas in mountainous regions were affected by topography. MSS bands were correlated with the effective incidence angle of solar illumination, which varies with topography. They found that the correlations were higher for the near-infrared bands than for the visible bands. In recent studies to correct digital MSS data for topographic effects, Kawata *et al.* (1988) and Civco (1989) mentioned that the near-infrared bands do have a higher correlation, or more noticeable topographic effects, and, therefore, more spatial variability in mountainous terrain covered with vegetation. The results presented in the preceding section, supported by the conclusions of these other studies, shows that the correlation of multispectral image data with spatial information that includes topographic variations is a function of wavelength, and that images collected in the near-infrared spectral band do have more spatial variability than those collected in the visible band. None of the sites used were in highly arid environments. However, from other studies, the correlation between the visible and near-infrared spectral bands in arid environments is known to be quite high (Chavez *et al.*, 1984; Chavez and Kwarteng, 1989). Therefore, the amount of spatial variability in the visible and near-infrared bands for images covering highly arid environments will probably be approximately the same. The near-infrared band may still be preferred, however, because the near-infrared band is affected less by the atmosphere than a band in the visible part of the spectrum, especially in arid environments. This may help keep the spatial variability higher in the near-infrared band. At the very least, the near-infrared band should be as good as the visible band in arid regions. Close inspection of the results generated with the Kenya image reveals only minor differences in the HPF in the bare soils areas. The fact that 65 percent of the image is covered by bare soils may be part of the reason that the curves of the near-infrared and visible bands shown in Table 3 are closer together than in the other images, especially because the topographic variations are small in the bare soils areas. However, image data covering several different types of arid environments need to be analyzed to confirm this observation. Moreover, the analyses of the mid-infrared bands 5 and 7 collected by the Landsat TM were not included in this paper because of the lack of these data in the SPOT system. However, a preliminary comparison with the Landsat TM visible and near-infrared bands indicates that the mid-infrared bands may have a higher spatial variability than either the visible or near-infrared bands. If so, this spectral region would be a good one to consider for applications dealing with spatial information. The extreme contrast between vegetated and nonvegetated areas will be present in these bands, similar to the visible bands, but the radiometric dynamic range is larger so that the local detail is not quantized away.

CONCLUSIONS

Both the statistical and visual results show that, for the six test sites used in this study, an image recorded in the near-infrared spectral band has more spatial variability than one recorded in the visible part of the spectrum. This difference is largest for densely vegetated areas: the more dense the vegetation is the larger will be the difference between the near-infrared and visible bands. Therefore, applications that require spatial variability information will generate better results with images collected in the near-infrared part of the spectrum rather than the visible part. In the future, designers of imaging systems that collect either a single higher resolution monochromatic image along with lower resolution multispectral images, such as the SPOT system currently does, or monochromatic images to be used for automatic correlation, such as for topographic extraction from stereo pairs, should consider using the near-infrared portion of the spectrum to collect these image data. It is recommended that further testing, including the analyses of images over arid regions and automatic image-to-image

correlation of stereo pairs using the visible and near-infrared bands, be done to help identify the specifications of future imaging systems. In the meantime, with data sets that currently exist, such as Landsat and SPOT multispectral and panchromatic images, users should consider using the single near- infrared band in their analyses that requires spatial variability information.

ACKNOWLEDGMENTS

The author would like to thank Miguel Velasco for his help in processing the data and generating the graphs shown in Tables 2 to 7.

REFERENCES

Chavez, P. S., Jr., S. C. Guptill, and J. Bowell, 1984. Image processing techniques for Thematic Mapper data. *Proceedings, American Society of Photogrammetry Spring Symposium*. Washington, D.C., pp. 728-752.

Chavez, P. S., Jr., and J. Bowell, 1988. Comparison of the spectral information content of Landsat Thematic Mapper and SPOT for three different sites in the Phoenix, Arizona Region. *Photogrammetric Engineering & Remote Sensing*, Vol. 54, No. 12, pp. 1699-1708.

Chavez, P. S., Jr., and A. Kwarteng, 1989. Extracting spectral contrast in Landsat Thematic Mapper image data using selective principal component analysis. *Photogrammetric Engineering & Remote Sensing*, Vol. 55, No. 3, pp. 339-348.

Civco, D. L., 1989. Topographic normalization of Landsat Thematic Mapper digital imagery. *Photogrammetric Engineering & Remote Sensing*, Vol. 55, No. 9, pp. 1303-1309.

Curran, P. J., 1988. The semivariogram in remote sensing: an introduction. *Remote Sensing of Environment*, Vol. 24, pp. 493-507.

Gallo, K. P., and J. C. Eidenshink, 1988. Differences in visible and near-ir responses, and derived vegetation indices, for the NOAA-9 and NOAA-10 AVHRRs: a case study. *Photogrammetric Engineering & Remote Sensing*, Vol. 54, No. 4, pp. 485-490.

Justice, C. O., S. W. Wharton, and B. N. Holben, 1981. Application of digital terrain data to quantify and reduce the topographic effect on Landsat data. *International Journal of Remote Sensing*, Vol. 2, No. 3, pp. 213-230.

Kawata, Y., S. Ueno, and T. Kusaka, 1988. Radiometric correction for atmospheric and topographic effects on Landsat MSS images. *International Journal of Remote Sensing*, Vol. 9, No. 4, pp. 729-748.

Teillet, P. M., B. Guindon, and D. G. Goodenough, 1982. On the slope-aspect correction of multispectral scanner data. *Canadian Journal of Remote Sensing*, Vol. 8, No. 2, pp. 84-106.

Townshend, J. R. G., and C. O. Justice, 1990. The spatial variation of vegetation changes at very coarse scales. *International Journal of Remote Sensing*, Vol. 11, No. 1, pp. 149-157.

Tucker, C. J., 1979. Red and photographic infrared linear combinations for monitoring vegetation. *Remote Sensing of Environment*, Vol. 8, pp. 127-150.

Woodcock, C. E., 1985. Variograms and spatial variation in remotely sensed images. *International Geoscience and Remote Sensing Symposium*, University of Massachusetts, Amherst, pp. 1078-1083.

Woodcock, C. E., and A. H. Strahler, 1987. The factor of scale in remote sensing. *Journal Remote Sensing of Environment*, Vol. 21, pp. 311-332.

(Received 10 June 1991; revised and accepted 22 November 1991)